Hindawi
Advances in Civil Engineering
Volume 2023, Article ID 3847003, 13 pages
https://doi.org/10.1155/2023/3847003

Research Article

Mechanical Properties and Mesostructure Evolution of Fibre-Reinforced Loess under Freeze-Thaw Cycles

Longfei Zhang,[1] **Zaiqiang Hu**,[1] **Hongru Li**,[1] **Haicheng She**,[2] **Xiaoliang Wang**,[1] **Xiaoning Han**,[1] **and Xi Yang**[1]

[1]*Institute of Geotechnical Engineering, Xi'an University of Technology, Xi'an 710048, China*
[2]*School of Urban Construction, Yangtze University, Jingzhou 434032, China*

Correspondence should be addressed to Zaiqiang Hu; huzq@xaut.edu.cn and Haicheng She; shehaicheng@126.com

Received 24 March 2023; Revised 29 April 2023; Accepted 2 May 2023; Published 27 October 2023

Academic Editor: Meng Gao

The strength of loess in seasonal frozen soil areas decreases evidently due to the freeze-thaw cycle, which even leads to some engineering and geological problems. Fibre reinforcement is very effective in improving the mechanical properties of soil. Triaxial tests under different water contents, freezing temperatures, and number of freeze-thaw cycles were carried out for fibre-reinforced loess to study the ability of fibre reinforcement to improve the resistance of loess to freeze-thaw damage; scanning electron microscopy (SEM) was also conducted. The effects of freeze and thaw deterioration and reinforcement were discussed by comparing the strength parameters under different test conditions, and the influence mechanism of freezing temperature, number of freeze-thaw cycles, and reinforcement on loess strength was explained. Results show that a lower freezing temperature indicates a more evident decrease in strength after thawing. Under the action of the first five freeze-thaw cycles, the degree of decrease is more prominent. The fibre reinforcement can reduce the fragmentation of aggregates in loess, thereby effectively restraining the deterioration effect of loess during freeze-thaw cycles. Finally, the strength parameter prediction model under different freeze-thaw cycles of reinforced loess is established, thereby providing theoretical support for engineering application and numerical simulation of fibre-reinforced loess.

1. Introduction

Loess is a loose sediment mainly formed by the wind. It was formed in the quaternary period and is a brownish-yellow silty clay. Generally, it has a uniform porous structure, mainly composed of quartz and feldspar [1, 2]. Loess is mainly distributed in arid and semiarid regions of Asia, Europe, and North and South America. According to statistics, the total area of loess in the world has reached 13 million·km^2, accounting for 9.3% of the land area. Among all loess regions, China's Loess Plateau is the most extensive, the thickest, and the most complete region in the world [3]. As shown in Figure 1, it is located in the northwest of China, with a length of approximately 1000 km from east to west and a width of approximately 800 km from north to south, including most of the areas east of Qinghai Province, north of Qinling Mountains, west of Taihang Mountains, and south of the Great Wall. In winter, the temperature in the north of the Loess Plateau can drop to −20°C, the maximum frozen soil depth can reach 160 cm, and the air above the plateau is thin. This condition results in remarkable differences in temperature during the day and night. The rainfall gradually increases from northwest to southeast. The maximum annual average rainfall can reach 750 mm, whereas the minimum annual rainfall is less than 200 mm.

A large part of China's loess plateau belongs to seasonally frozen regions. With the economic development of these regions, many large-scale engineering projects have been carried out, and some geotechnical problems, such as landslides [4], ground collapse [5], and soil erosion [6] have occurred during the construction process, as shown in Figure 2. The strength is very high in the dry state due to the prominent structural properties of loess. As shown in Figure 3, the vertical height can reach 20 meters to 30 meters

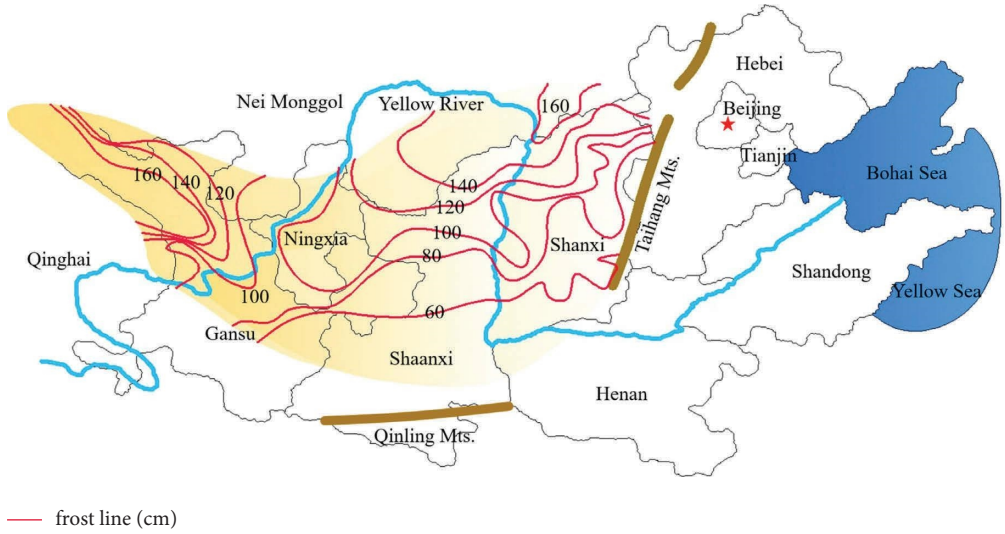

Figure 1: Distribution of loess in China and standard frost line.

and remain stable, but the strength is significantly reduced when immersed. Some special loess can produce collapse deformation even under the action of its weight when it encounters water. When the deformation of slopes, channels, airports, and highway subgrades is extremely large, geological disasters and threats to pedestrian safety are highly probable.

In the freeze-thaw cycle, water in the soil alternately transforms between liquid and solid. As shown in Figure 4, the volume of water in the soil expands from liquid to solid, destroying the soil's cementitious substances. When the ice melts, the soil collapses due to the loss of the support of the ice crystals. At present, studies on the effect of freezing and thawing on the mechanical properties of soil are abundant. For example, through a large number of field investigations, the damage induced by freeze-thaw cycles is divided into erosion damage, peeling damage, and thawing damage, and the mechanism of bank slope instability caused by these cycles is revealed [7–9]. The changes in pores and fractal dimensions during the freeze-thaw process were studied by the scanning electron microscope (SEM) [10]. Some scholars studied the morphological characteristics of soil surface cracks from the perspectives of soil type, water content, and freeze-thaw cycles [11, 12]. Other scholars studied the freeze-thaw characteristics of lime-stabilised soil and cement-stabilised soil [13, 14]. Although some effects have been achieved, the cost is high, and the ecological impact is great.

The reinforcement technology, which was proposed in the 1970s, is simple in operation and low in cost; it has been widely used in geotechnical protection. The reinforcement materials initially used are steel bars, geogrids, and geotextiles. The disadvantages of these materials include the directional reinforcement and easy formation of a potential sliding layer [15]. Fibre reinforcement, on the contrary, incorporates fibre evenly into the soil to avoid the formation of a weak layer [16]. Many scholars have tried various fibre reinforcements to improve soil strength, such as palm fibre [17], lignin fibre [18], and waste fibres from blankets and nylon cloth [19]. Inspired by these studies, our team proposed to enhance the freeze-thaw resistance of loess by using fibre reinforcement, adding polypropylene fibre to loess, verifying the effect by triaxial test, explaining the mechanism by SEM test, and finally establishing the strength parameter prediction model of reinforced fibre under the freeze-thaw cycle. The present study provides support for engineering reinforcement construction and simulation of reinforced loess.

2. Test Materials and Protocols

2.1. Soil for Testing. The soil used in the test is Q_3 Malan loess obtained from the northern suburbs of Xi'an, with a depth of 6-7 m, yellowish-brown colour, no bedding, uniform texture, and relatively hard texture. The soil sample has no calcareous nodules, with a few wormholes, shells, and tree roots. The basic physical parameters are shown in Table 1. The soil with a plastic index between 10 and 17, and a certain clay content is silty clay.

2.2. Reinforced Fibre for Testing. In the test, polypropylene fibre is selected as the reinforcing material. As shown in Figure 5, this fibre has low cost, good chemical stability, is not easily corroded, has little impact on the environment, and has high tensile strength, suitable for adding loess to improve its freeze-thaw resistance. Its principal physical properties are shown in Table 2.

2.3. Sample Preparation. When the test soil was retrieved from the site, it was bound and sealed with black plastic and stored in the laboratory for future use. The test soil was initially crushed, and the large particle impurities were removed using a 2 mm aperture sieve. After many attempts, we found that the fibre can mix with the soil evenly when the moisture content is lower than 10%. Therefore, prior to sample preparation, the soil mass was air-dried to a lower moisture content, and then the fibre was added to the corresponding moisture content by a watering pot; a plastic

(a) (b) (c)

Figure 2: Common types of disasters in the loess area: (a) loess landslides; (b) ground collapse; (c) soil erosion.

Figure 3: Loess gully in the nearly vertical state.

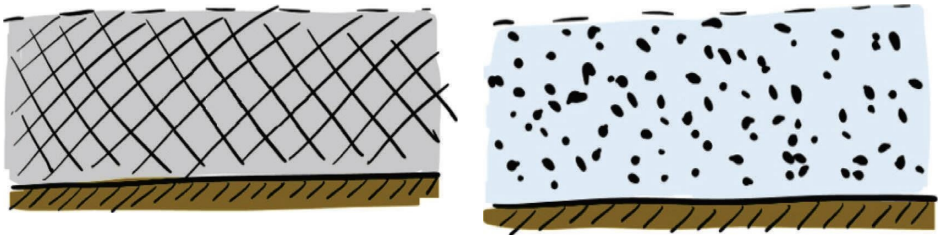

(a) (b)

Figure 4: Loess in freeze-thaw environment: (a) frozen loess; (b) melted loess.

Table 1: Basic physical parameters of test soil.

Specific gravity of soil particles G_s	Natural dry density ρ_d (g/cm^{-3})	Maximum dry density ρ_d (g/cm^{-3})	Optimum moisture content ω (%)	Plastic limit ω_p (%)	Liquid limit ω_L (%)	Plasticity index I_p
2.70	1.32	1.60	17.8	15.3	26.6	11.3

wrap was used to cover it to prevent water evaporation. The soil samples were stored for 24 hours to ensure uniform moisture. The samples were prepared by layered compaction and placed into a controllable high-and low-temperature test chamber for a freeze-thaw cycle test. The operation process is shown in Figure 6.

2.4. Test Schemes. Three groups of water contents, namely, 17.8%, 22%, and saturated water content were selected for the tests. The dry density of the sample was 1.52 g/cm^3 according to the compaction degree of 95%, and the size was Ø39.1 × 80 mm. In accordance with the test results of Zhu et al. [20], the fibre length of 12 mm and the incorporation ratio of 0.5% were selected for this experiment. The SYL-2 stress–strain path triaxial instrument was adopted as the test instrument. The specific test plan, shown in Tables 3–5, can be divided into three parts. The first part mainly studies the effect of freezing temperature on the mechanical properties of unreinforced/reinforced loess. The second part mainly studies the mechanical properties of unreinforced/reinforced loess after melting and compares them with those in the first part of the experiment. The third part mainly studies the effect of freeze-thaw cycles on the mechanical properties of unreinforced/reinforced loess.

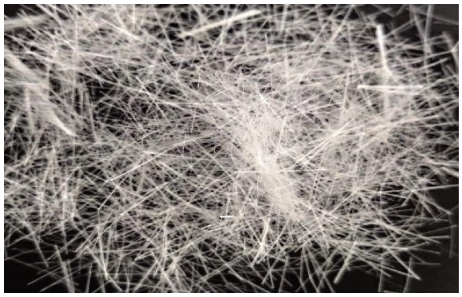

Figure 5: Reinforced fibre material.

Table 2: Physical parameters of polypropylene fibre.

Type of fibre	Diameter (μm)	Elastic modulus E (GPa)	Tensile strength f (MPa)	Dispersion	Acid and alkali resistance
Bundled monofilament	20–50	>3.5	>480	Good	Very good

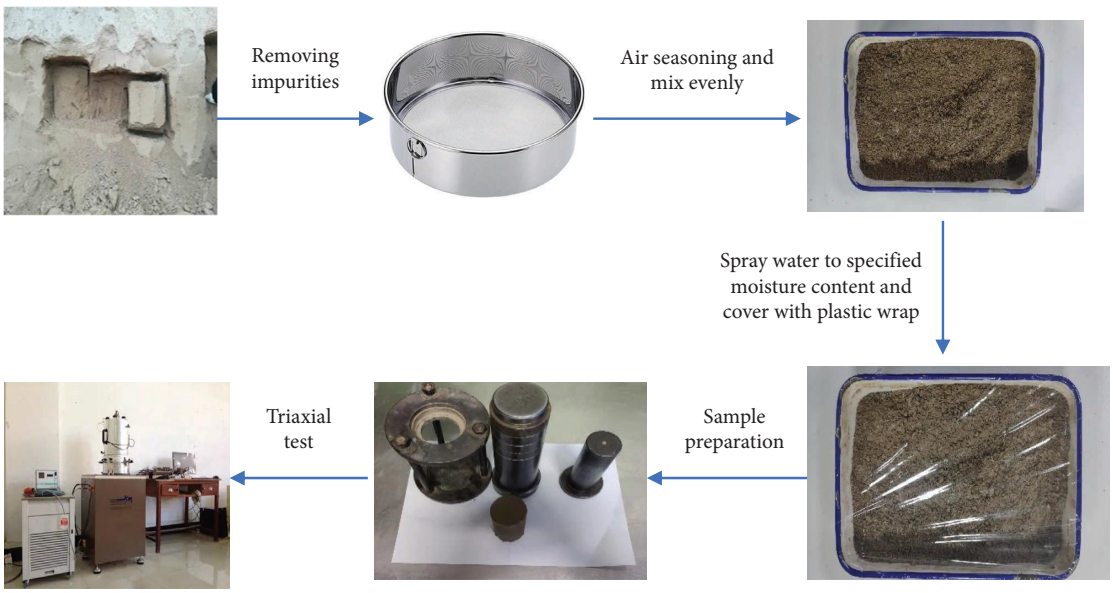

Figure 6: Test procedures.

Table 3: Influence of freezing temperature on mechanical properties of reinforced loess.

Fibre reinforcement conditions	Sample moisture content	Temperature	Time	Shear method
Unreinforced Reinforced	17.8% 22% Saturated	−10°C −5°C 0°C 5°C	48 h	Unconsolidated and undrained shear

3. Test Results and Analysis

3.1. Influence of Freezing Temperature on Strength Parameters of Unreinforced/Reinforced Loess. The variation of strength parameters of reinforced and unreinforced loess at different freezing temperatures is shown in Figures 7 and 8.

Figure 7(a) shows that the cohesion decreases when the water content increases without freezing. The reason is that the optimal water content is initially used in this test, the sample reaches the water content corresponding to the maximum dry density in the compaction test, and this water content enables the cementing material in the sample to

Table 4: Influence of melting on mechanical properties of reinforced loess.

Fibre reinforcement conditions	Sample moisture content	Freezing temperature	Freezing time	Melting temperature	Melting time	Shear method
Unreinforced Reinforced	17.8% 22% Saturated	−10°C −5°C 0°C	48 h	5°C	24 h	Unconsolidated and undrained shear

Table 5: Influence of the number of freeze-thaw cycles on mechanical properties of reinforce loess.

Fibre reinforcement conditions	Sample moisture content	Freeze-thaw method	Freeze-thaw cycles	Shear method
Unreinforced Reinforced	17.8% 22% Saturated	Freeze at −10°C for 24 h, thaw at 10°C for 24 h	0, 1 3, 5 7, 9 12	Consolidated and drained shear

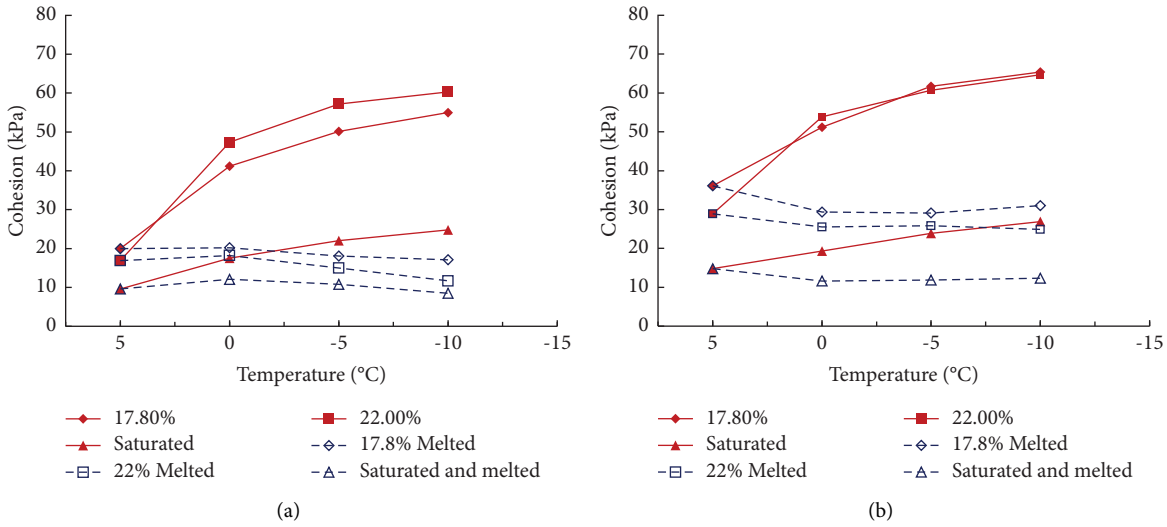

Figure 7: Variation of cohesion at different freezing temperatures: (a) unreinforced loess; (b) reinforced loess.

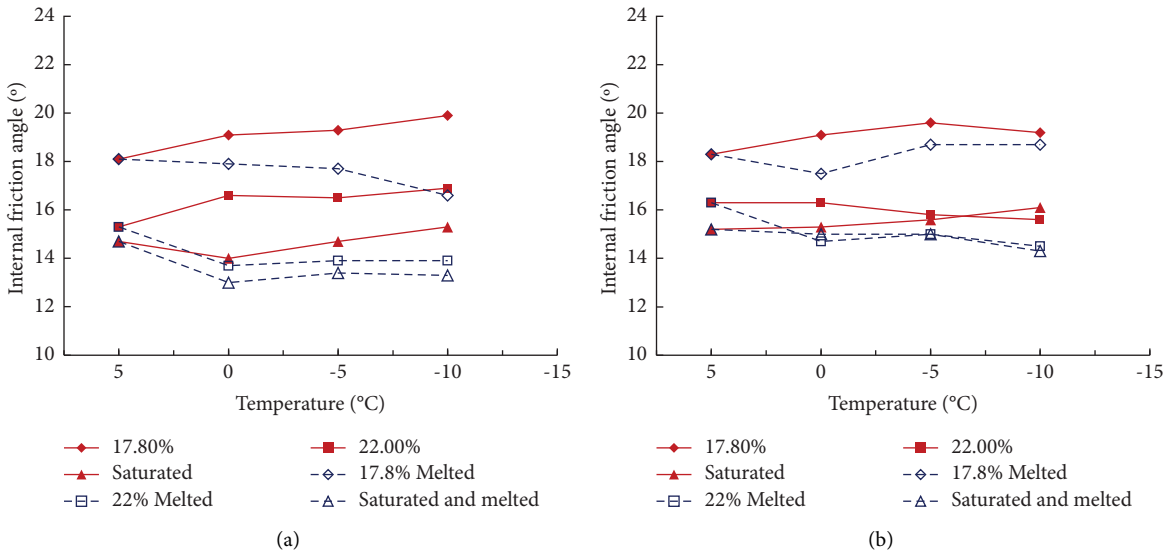

Figure 8: Variation of internal friction angle at different freezing temperatures: (a) unreinforced loess; (b) reinforced loess.

better connect the soil particles. When the water content further increases, the water film wrapped by the soil particles becomes thicker, and the bonding force between particles and matric suction becomes weaker, decreasing the cohesion of the sample.

The test results show that freezing and thawing have a deteriorating effect on the strength of loess. During the freezing process, the pore water in the sample is converted into ice, and the volume expands, thereby causing the sample to expand. The sample shrinks and settles when the ice in the sample melts, destroying the original bonding and occlusal form of the sample. As a result, cohesion decreases.

Figure 7(b) shows that the cohesion of the reinforced samples with 17.8%, 22% and saturated water contents at 5°C is 36.1, 28.9, and 14.8 kPa, respectively; compared with the unreinforced samples, the increase was 80%, 71%, and 54%. The high water content is not conducive to fibre reinforcement. The cohesion of the reinforced sample after freezing is also improved compared with that of the unreinforced samples. Although the cohesion of the frozen sample decreases after melting, it is still higher than that of the unstiffened sample. The main reason is that the sample achieves a more robust structure given the existence of fibre, limiting the expansion of the sample during freezing and reducing the deterioration effect of freezing and thawing.

Figures 8(a) and 8(b) show that after freezing and thawing, the internal friction angle of the unreinforced samples decreases, basically within 20%. The internal friction angle of the reinforced sample also changes but is not evident, and the variation range is within 10%. The test results show that a single freeze-thaw slightly affects the internal friction angle of the sample because the friction strength of loess is mainly affected by particle size gradation, particle shape, and mineral composition, and a single freeze-thaw

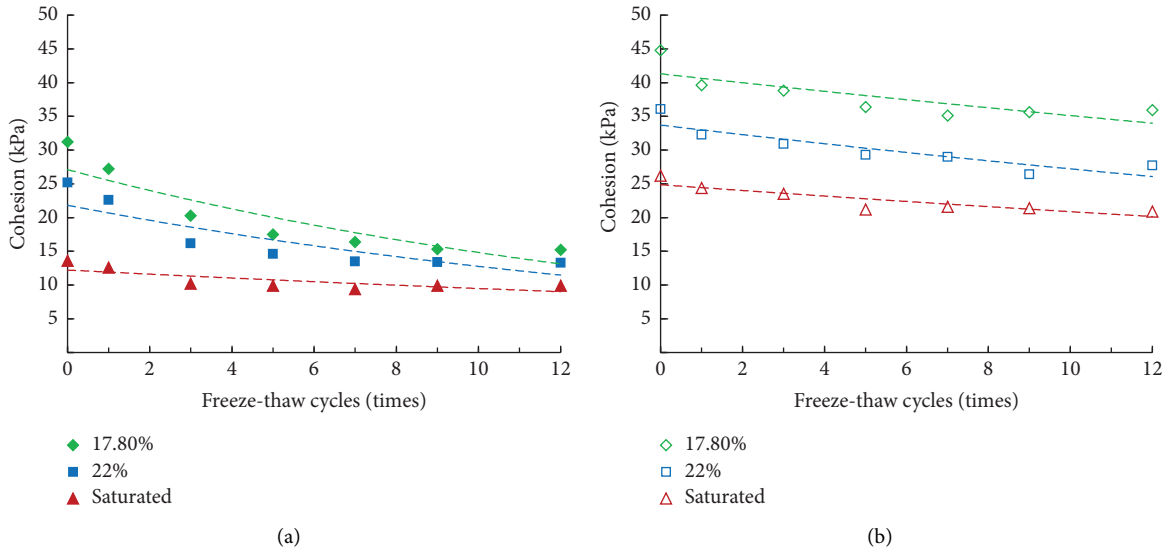

Figure 9: Variation of cohesion under different freeze-thaw cycles: (a) unreinforced loess; (b) reinforced loess.

has limited effect on loess. Fibre reinforcement has a limited increase in the internal friction angle of the sample, but it can reduce the attenuation of the internal friction angle under freeze-thaw action.

3.2. Influence of Freeze-Thaw Cycles on Strength Parameters of Unreinforced/Reinforced Loess. Figure 9(a) shows that the cohesion of the unreinforced sample decreased significantly under the action of the first five freeze-thaw cycles. When the number of freeze-thaw cycles exceeds five times, the change in cohesion tends to be stable. Freeze-thaw cycles have little effect on saturated samples. Comparing Figure 9(b), we can find that the cohesion of the sample increases significantly after being reinforced, and after 12 freeze-thaw cycles, the cohesion of the samples with 17.8%, 22%, and saturated water content is 35.9 kPa, 27.7 kPa, and 20.9 kPa, respectively, which are increased by 130%, 97%, and 111% compared with the unreinforced samples The test results show that fibre reinforcement can significantly improve the cohesion of loess. The reason is that the fibres and soil particles are intertwined and wrapped, significantly enhancing the cementation between particles. Fibre enables the soil to maintain a high strength after multiple freeze-thaw cycles.

Figures 10(a) and 10(b) show that under the freeze-thaw cycle's action, the sample's internal friction angle decreases slightly. Still, the change is not apparent, indicating that the freeze-thaw process slightly affects the internal friction angle.

According to the previous analysis, the freeze-thaw cycle mainly reduces the cohesion of the undisturbed loess, that is, the cementing force between particles, whereas the reinforcement effect counteracts the deterioration of the freeze-thaw effect by enhancing the structural integrity of the soil. Table 6 shows the cohesion deterioration table of unreinforced/reinforced samples under freeze-thaw action. Δ and w are calculated using formulas (1) and (2), respectively.

$$\Delta_i = c_{i-1} - c_i, \tag{1}$$

$$w_i = \frac{\Delta_i}{\sum_{i=1}^{6} \Delta_i} \times 100, \tag{2}$$

where c_i is the cohesion force after the i-level freeze-thaw cycle.

The finding shows that the first five freeze-thaw cycles have the most significant impact on the cohesion of loess. Under the action of the first five freeze-thaw cycles, the cohesion of the sample decreased by 80%, and the strength parameters and freeze-thaw resistance of the sample were improved after reinforcement.

3.3. Strength Parameter Prediction Model. According to the changing trend of loess cohesion and internal friction angle under freeze-thaw cycles, a calculation model for the change in strength parameters of reinforced loess with the number of freeze-thaw cycles is established. Four parameters are introduced into the model, S_c and S_φ are the strengthening coefficients under loess reinforcement, K_c and K_φ are the deterioration coefficients under freeze-thaw action, and the calculation methods are as follows:

$$\begin{aligned} S_c &= \frac{c_{d0}}{c_{u0}}, \\ S_\varphi &= \frac{\varphi_{d0}}{\varphi_{u0}}, \\ K_c &= \frac{c_{dn}}{c_{d0}}, \\ K_\varphi &= \frac{\varphi_{dn}}{\varphi_{d0}}, \end{aligned} \tag{3}$$

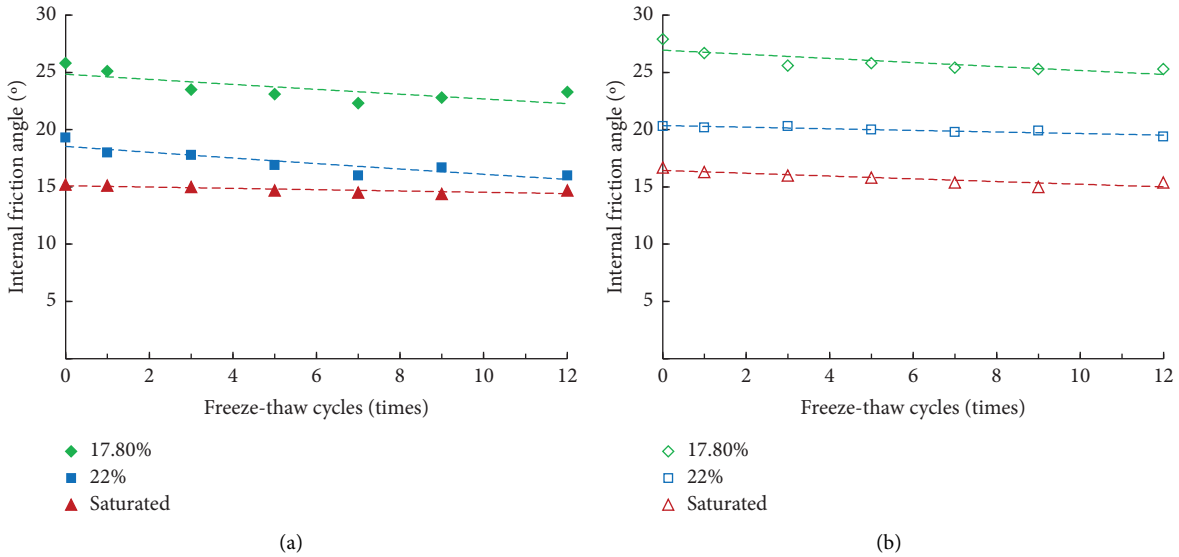

Figure 10: Variation of internal friction angle under different freeze-thaw cycles: (a) unreinforced loess; (b) reinforced loess.

Table 6: Cohesion deterioration rate of reinforced/unreinforced loess under freeze-thaw cycles.

Level of freeze-thaw cycles	Water content 17.8%				Water content 22%				Water content saturated			
	Unreinforced		Reinforced		Unreinforced		Reinforced		Unreinforced		Reinforced	
	Δ (kPa)	w (%)	Δ (kPa)	w (%)	Δ (kPa)	w (%)	Δ (kPa)	w (%)	Δ (kPa)	w (%)	Δ (kPa)	w (%)
1	4.0	25.0	5.2	58.4	2.6	21.8	3.8	45.2	1.0	27.0	1.8	33.9
2	6.9	43.1	0.8	8.9	6.4	53.7	1.4	16.6	2.4	64.8	0.9	16.9
3	2.8	17.5	2.4	26.9	1.6	13.4	1.6	19.0	0.3	8.1	2.3	43.4
4	1.1	6.8	1.3	14.6	2.0	16.8	0.3	3.5	0.5	13.5	−0.4	−7.5
5	1.1	6.8	−0.5	−5.6	0.1	0.8	2.6	30.9	−0.5	−13.5	0.2	3.7
6	0.1	0.6	−0.3	−3.3	0.1	0.8	−1.3	−15.4	0	0	0.5	9.4

where c_{u0} and φ_{u0} are the cohesion and internal friction angle of the frozen-thawed sample of the unreinforced loess, respectively; c_{d0} and φ_{d0} are the cohesion and internal friction angle of the frozen-thawed sample of the reinforced loess, respectively; c_{dn} and φ_{dn} are the cohesion and internal friction angle of the reinforced loess after n freeze-thaw cycles.

The influence of different water contents can be avoided, and the strength parameters of the reinforcement after freezing and thawing can be determined given that the strengthening coefficient and deterioration coefficient are the ratios of the same water content. We can obtain the strengthening coefficients $S_c = 1.6$ and $S_\varphi = 1.1$, considering the average value of the strengthening coefficients with different water contents, and the average strength deterioration coefficients are shown in Table 7.

The average strength parameter of deterioration coefficients under different freeze-thaw cycles in Table 7 is exponentially fitted, and Figure 11 shows the fitting curve. Formulas (4) and (5) are used to quantitatively calculate the strength parameters of reinforced loess under any number of freeze-thaw cycles, providing data support for the numerical simulation of the shear strength of reinforced loess.

$$c_{dn} = 1.6 \times 0.98e^{-0.006n} \times c_{u0}, \quad (4)$$

$$\varphi_{dn} = 1.1 \times 0.93e^{-0.018n} \times \varphi_{u0}. \quad (5)$$

4. Microscopic Mechanism Analysis of Fibre Reinforcement

Figure 12 shows that a small amount of clay particles are attached to the initially smooth fibre surface. When the soil sample is subjected to shear deformation or failure under load, the fibres in the soil undergo a state of tension, which constrains the further deformation of the soil. When the stress exceeds the adhesion and friction force between clay particles and the fibre surface, the fibres mismove with the soil particles or are even pulled out. Similar to a tree's root, the fibre can disperse the external load to other areas, reduce the stress concentration, and thus enhance the strength of the sample.

Figures 13(a)–13(h) show SEM images of unreinforced/reinforced loess under different freeze-thaw cycles. Figures 13(a), 13(c), 13(e) and 13(g) show SEM images of the unreinforced loess samples under different freeze-thaw

Table 7: Average strength parameter deterioration coefficient.

Deterioration factor	Freeze-thaw cycles						
	0	1	3	5	7	9	12
K_c	1	0.90	0.87	0.81	0.80	0.78	0.78
K_φ	1	0.97	0.96	0.95	0.94	0.93	0.93

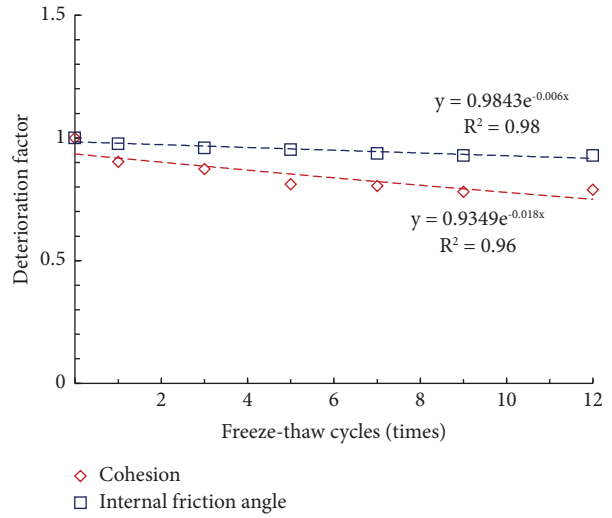

Figure 11: Average strength parameter degradation coefficient curve.

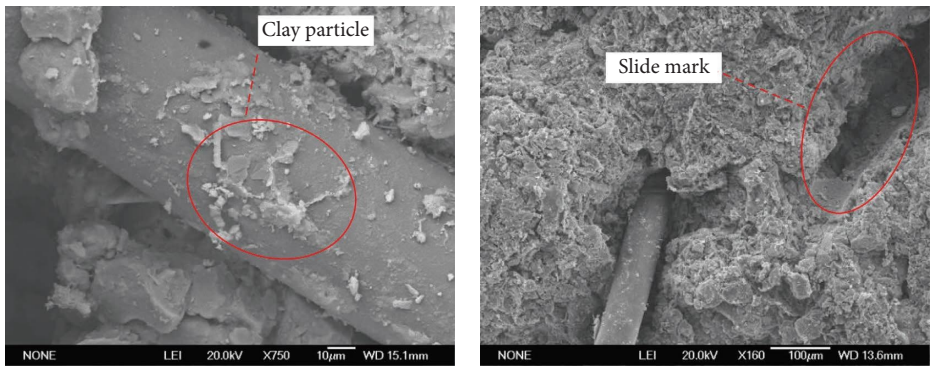

(a) (b)

Figure 12: Micrograph of fibre reinforcement action: (a) fibre surface; (b) slip mark where the fibres have been pulled out.

cycles. Prior to freeze-thaw, the skeleton particles of the tested loess were mainly composed of cementitious aggregates, single round particles, and sheet-like particles, and the particles were closely embedded in a granular, agglomerated, embedded, and cementitious structure. After multiple freeze-thaw cycles, the microstructure characteristics changed remarkably, and the number of large skeleton particles of the loess decreased significantly; they became loose, with an increase in small pores. The reason for this phenomenon is that the growth of internal ice crystals increases the pore volume of the sample during the freezing process of the sample, thereby squeezing the skeleton particles. Figures 13(b), 13(d), 13(f), and 13(h) show SEM images of reinforced loess samples under different freeze-thaw cycles. The figure shows that samples without freeze-thaw cycles have larger internal pores. Microcracks appear around some pellets during the initial freeze-thaw process. As the number of freeze-thaw cycles increases, microcracks further develop, ultimately leading to pellet fragmentation. The large pores are gradually filled with fragmented aggregates, and the large pores in the sample transform into small pores. Some aggregates originally in contact with the surface transform into point contacts, weakening connections between particles. The comparison between Figures 13(g) and 13(h) indicates that the degree of fragmentation of the reinforced sample is weaker than that of the unreinforced sample.

The SEM image extracted by the edge detection technology of the canny operator and the pores are divided into micropores ($S < 20\,\mu m^2$), small pores ($20\,\mu m^2 \le S < 100\,\mu m^2$), mesopores ($100\,\mu m^2 \le S < 300\,\mu m^2$), and macro pores ($S \ge 300\,\mu m^2$). Figures 14(a) and 14(b) are

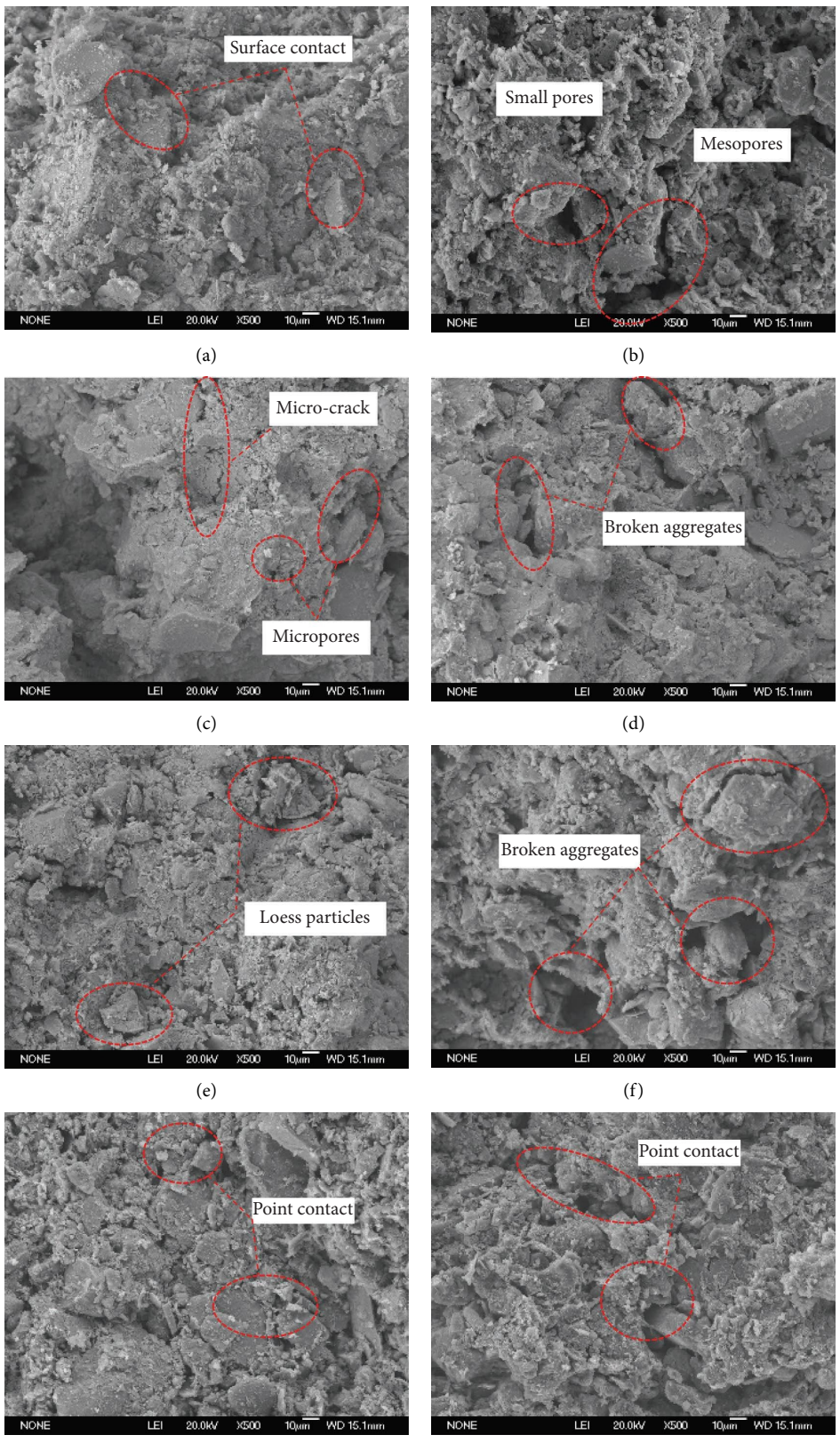

Figure 13: Average strength parameter degradation coefficient curve: (a) unreinforced, no freeze-thaw cycle; (b) reinforced, no freeze-thaw cycle; (c) unreinforced, one freeze-thaw cycle; (d) reinforced, one freeze-thaw cycle; (e) unreinforced, five freeze-thaw cycles; (f) reinforced, five freeze-thaw cycles; (g) unreinforced, 12 freeze-thaw cycles; (h) reinforced, 12 freeze-thaw cycles.

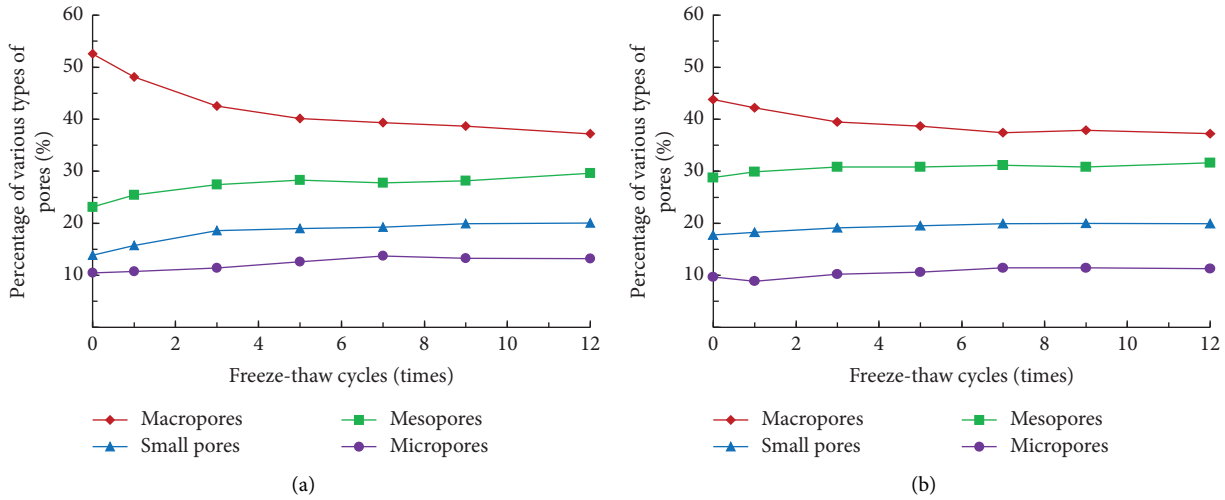

Figure 14: Variation curves of pore proportions of different types: (a) unreinforced loess; (b) reinforced loess.

the ratios of various pore areas to the total pore area under different freeze-thaw cycles. The proportion of large pores in unreinforced loess decreased significantly under the action of freeze-thaw cycles, mainly transformed into mesopores and small pores. The decrease in the proportion of large pores in reinforced loess is significantly smaller than those in the unreinforced loess, indicating that the aggregates are less broken, and reinforcement can reduce the deterioration effect of freezing and thawing.

5. Conclusions

(1) When the initial water content is the same, lower freezing temperature indicates higher cohesion and smaller increase in the angle of internal friction. The cohesion decreases significantly as the ice crystals in the sample melt, and fibre reinforcement can reduce the freeze-thaw damage of loess.

(2) Under the conditions of freeze-thaw cycles, the cohesion of loess deteriorated significantly in the first five freeze-thaw cycles, and the strength parameters tended to be stable in the subsequent period. Fibre reinforcement improves the overall structure, inhibits expansion and subsidence caused by freeze-thaw cycles, and enhances the ability of the sample to resist freeze-thaw cycle damage by wrapping and connecting with soil particles.

(3) The strength parameter prediction model of fibre-reinforced loess under freeze-thaw cycles was established through the test data, which supported parameter selection in numerical simulation.

(4) According to the pore area, the pores are divided into four types. SEM test and image processing technology show that the freeze-thaw cycle leads to the breakage of the agglomerates, the transformation of large pores to mesopores and small pores, and the fibre reinforcement can restrain the breakage of the agglomerates.

Data Availability

The data used to support the findings of this study are included within the article.

Conflicts of Interest

The authors declare that they have no conflicts of interest.

Authors' Contributions

Zhang Longfei proposed ideas and performed experiments. Li Hongru and She Haicheng designed the test's content, method, and technical route and combined it with the actual situation to determine the test scheme. Wang Xiaoliang, Han Xiaoning, and Yang Xi assisted with materials and background knowledge. Hu Zaiqiang reviewed and edited the manuscript. All authors have read and agreed to the published version of the manuscript.

Acknowledgments

This work was supported by the National Natural Science Foundation of China (No. 52274007) and the Science and Technology Innovation Project of Key Laboratory of Shaanxi Province China (No. 2014SZS15-Z02), which are gratefully acknowledged.

References

[1] X. Ma and H. Jiang, "Combined tectonics and climate forcing for the widespread aeolian dust accumulation in the Chinese Loess Plateau since the early late miocene," *International Geology Review*, vol. 57, no. 14, pp. 1861–1876, 2015.

[2] Y. Li, W. Shi, A. Aydin, M. A. Beroya-Eitner, and G. Gao, "Loess genesis and worldwide distribution," *Earth-Science Reviews*, vol. 201, 2020.

[3] Y. Zhu, X. Jia, J. Qiao, and M. Shao, "What is the mass of loess in the Loess Plateau of China?" *Science Bulletin*, vol. 64, no. 8, pp. 534–539, 2019.

[4] S. Ma, H. Qiu, S. Hu et al., "Quantitative assessment of landslide susceptibility on the Loess Plateau in China," *Physical Geography*, vol. 41, no. 6, pp. 489–516, 2020.
[5] L.-S. Deng, W. Fan, Y.-P. Yin, and Y.-B. Cao, "Case study of a collapse investigation of loess sites covered by very thick loess–paleosol interbedded strata," *International Journal of Geomechanics*, vol. 18, no. 11, Article ID 05018009, 2018.
[6] X. Wen, "Temporal and spatial relationships between soil erosion and ecological restoration in semi-arid regions: a case study in northern Shaanxi, China," *GIScience and Remote Sensing*, vol. 57, no. 4, pp. 572–590, 2020.
[7] S. B. Xie, Q. Jian-jun, L. Yuan-ming, Z. Zhi-wei, and X. Xiang-tian, "Effects of freeze-thaw cycles on soil mechanical and physical properties in the qinghai-tibet plateau," *Journal of Mountain Science*, vol. 12, no. 4, pp. 999–1009, 2015.
[8] J. Xu, Z. Q. Wang, J. W. Ren, S. H. Wang, and L. Jin, "Mechanism of slope failure in loess terrains during spring thawing," *Journal of Mountain Science*, vol. 15, no. 4, pp. 845–858, 2018.
[9] Z. P. Qin, Y. M. Lai, Y. Tian, and M. Y. Zhang, "Effect of freeze-thaw cycles on soil engineering properties of reservoir bank slopes at the northern foot of tianshan mountain," *Journal of Mountain Science*, vol. 18, no. 2, pp. 541–557, 2021.
[10] C. Han and P. Cheng, "Micropore variation and particle fractal representation of lime-stabilised subgrade soil under freeze–thaw cycles," *Road Materials and Pavement Design*, vol. 16, no. 1, pp. 19–30, 2015.
[11] K. Xing, Z. Zhou, H. Yang, and B. Liu, "Macro–meso freeze–thaw damage mechanism of soil–rock mixtures with different rock contents," *International Journal of Pavement Engineering*, vol. 21, no. 1, pp. 9–19, 2020.
[12] J. Yue, X. Huang, L. Zhao, and Z. Wang, "Study on the factors affecting cracking of earthen soil under dry shrinkage and freeze–thaw conditions," *Scientific Reports*, vol. 12, no. 1, pp. 1816–1821, 2022.
[13] G. Tebaldi, M. Orazi, and U. S. Orazi, "Effect of freeze—thaw cycles on mechanical behavior of lime-stabilized soil," *Journal of Materials in Civil Engineering*, vol. 28, no. 6, Article ID 06016002, 2016.
[14] H. S. Sahlabadi, M. Bayat, M. Mousivand, and M. Saadat, "Freeze–thaw durability of cement-stabilized soil reinforced with polypropylene/basalt fibers," *Journal of Materials in Civil Engineering*, vol. 33, no. 9, Article ID 04021232, 2021.
[15] C. Li and J. G. Zornberg, "Mobilization of reinforcement forces in fiber-reinforced soil," *Journal of Geotechnical and Geoenvironmental Engineering*, vol. 139, no. 1, pp. 107–115, 2013.
[16] Z. Gao and J. Zhao, "Evaluation on failure of fiber-reinforced sand," *Journal of Geotechnical and Geoenvironmental Engineering*, vol. 139, no. 1, pp. 95–106, 2013.
[17] J. Qu and H. Zhu, "Function of palm fiber in stabilization of alluvial clayey soil in yangtze river estuary," *Journal of Renewable Materials*, vol. 9, no. 4, pp. 767–787, 2021.
[18] M. E. Orakoglu, J. Liu, R. Lin, and Y. Tian, "Performance of clay soil reinforced with fly ash and lignin fiber subjected to freeze-thaw cycles," *Journal of Cold Regions Engineering*, vol. 31, no. 4, Article ID 04017013, 2017.
[19] Y. Wang, "Utilization of recycled carpet waste fibers for reinforcement of concrete and soil," *Polymer-Plastics Technology and Engineering*, vol. 38, no. 3, pp. 533–546, 1999.
[20] M. Zhu, W. Ni, X. Li, H. Wang, and L. Zhao, "Study on unconfined compressive strength and deformation after incorporating polypropylene fiber into loess," *Science Technology and Engineering*, vol. 20, no. 20, pp. 8337–8343, 2020.